ORIGINAL RESEARCH

HER2 and APC Mutations Promote Altered Crypt-Villus Morphology and Marked Hyperplasia in the Intestinal Epithelium

Elisa Murray,[1,2] Xiaoqing Cheng,[2] Anagha Krishna,[2] Xiaohua Jin,[2] Takahiro E. Ohara,[3] Thaddeus S. Stappenbeck,[5] and Ron Bose[2,4]

[1]Division of Biology and Biomedical Sciences, Department of Biochemistry, Washington University School of Medicine in St. Louis, St. Louis, Missouri; [2]Division of Oncology, Department of Medicine, Washington University School of Medicine in St. Louis, St. Louis, Missouri; [3]Department of Pathology and Immunology, Washington University School of Medicine in St. Louis, St. Louis, Missouri; [4]Alvin J. Siteman Cancer Center, Washington University School of Medicine in St. Louis, St. Louis, Missouri; and [5]Department of Inflammation and Immunity, Lerner Research Institute, Cleveland Clinic, Cleveland, Ohio
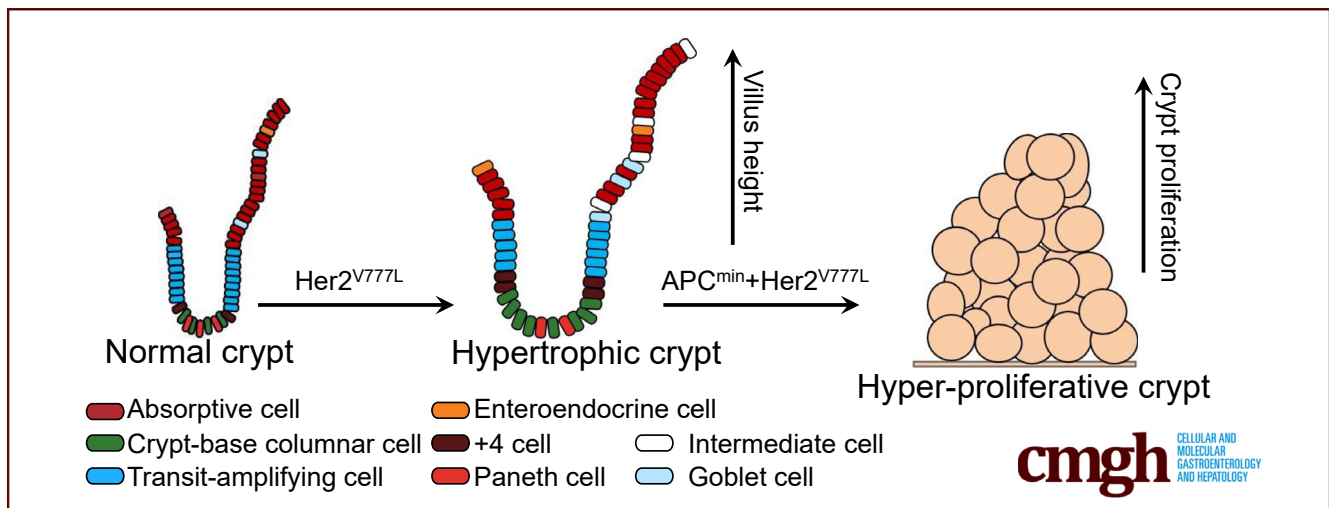
SUMMARY

We developed a transgenic mouse expressing the HER2^{V777L} activating mutation in the intestines. HER2^{V777L} expression resulted in hypertrophic crypt formation, hyperplasia, and intermediate cell formation on intestinal villi. Mutation of both APC and HER2 enhanced proliferation of intestinal crypts.

BACKGROUND AND AIMS: The Cancer Genome Atlas (TCGA) project has identified HER2 mutations or amplification in 7% of colon cancers. In addition to HER2 mutations, colon cancer patients also possess co-occurring mutations in genes such as APC. Here, we investigated the role of HER2 and APC mutations on the crypt-villus architecture of the intestinal epithelium, localization of secretory cells, and expression of intestinal stem cell markers.

METHODS: We generated a HER2 transgenic mouse (HER2^{V777L} Tg) possessing an activating mutation commonly found in colorectal cancer patients, HER2^{V777L}, using transcription activator-like effector nucleases–based gene editing technology. We expressed the HER2^{V777L} transgene in mouse small intestine and colon using Lgr5-Cre and Villin-Cre recombinases. In addition, we analyzed Lgr5-Cre; APC^{min}; HER2^{V777L} Tg mice by morphologic and gene expression assays on intestinal sections and organoids derived from the epithelium.

RESULTS: HER2^{V777L} expression resulted in hypertrophic crypt formation with expanded zones of proliferation. Proximal intestinal villi showed increased abundance of multiple differentiated lineages including extensive intermediate cell differentiation, as evidenced by MUC2/MMP7 co-immunofluorescence and transmission electron microscopy. HER2^{V777L} expression in the context of APC loss resulted in further enhancement and expansion of the proliferative crypt compartment.

CONCLUSIONS: We established an epithelial intrinsic role for HER2^{V777L} on enhanced cellular proliferation. Additionally, we determined that HER2 and APC mutations, when combined, promote enhanced proliferation of intestinal crypts. *(Cell Mol Gastroenterol Hepatol 2021;12:1105–1120; https://doi.org/10.1016/j.jcmgh.2021.04.012)*

The intestinal epithelium is tightly regulated by the expression of several growth factors produced within the stem cell niche that control intestinal cell proliferation and differentiation. For example, members of the epidermal growth factor receptor (EGFR) family (human epidermal growth factor receptor 2 [HER2], HER3, and HER4) are commonly expressed throughout the intestinal epithelium and regulate cell migration, survival, and differentiation.[1] Furthermore, overexpression of these receptor tyrosine kinases is known to result in poor outcomes in several gastric and other solid tumors types.[2,3] Further study of these receptor tyrosine kinases is needed to delineate their role in cancer development.

Recent studies by The Cancer Genome Atlas colorectal cancer project have identified 7% of colorectal cancer (CRC) patients with HER2 mutations or amplification.[4] In vitro characterization of HER2 mutations has identified several activating mutations, such as V777L and V842I that activate downstream signaling pathways in colon cancer cell lines and confer anchorage-independent growth in soft agar assays.[5] As a result, HER2 mutations are thought to play a crucial role in cancer development; however, the precise role that these mutations play on the intestinal epithelium has not been determined.

Prior studies on EGFR family members have determined that these receptors play crucial roles in promoting growth and proliferation. For example, in vivo expression of EGFR was found to be crucial for promoting intestinal cell proliferation and tumor initiation.[6] Additionally, expression of HER3 in the intestinal epithelium has been found to promote wound healing following chemically induced colitis, tumorigenesis, and differentiation of secretory cell types, such as Paneth cells.[7–9] Similarly, studies examining the role of HER2 expression in the intestinal epithelium have identified that HER2 plays a role in recovery of chemically induced colitis.[7] However, additional in vivo studies of HER2 are limited and the role of an activating HER2 mutation on intestinal epithelial architecture has not been previously determined. As a result, we sought to determine the role of an activating HER2 mutation, HER2^{V777L}, on the crypt-villus architecture of the intestinal epithelium. Additionally, we also characterized gene expression changes in stem cells and secretory marker genes induced by expression of our HER2^{V777L} transgene. Last, we also sought to examine the role of HER2^{V777L} on tumor formation and CRC progression using an APC^{min} mouse model.

We demonstrated that in vivo expression of HER2^{V777L} in the proximal small intestine resulted in hyperplasia, expansion of intestinal crypts, increased expression of stem cell markers, and intermediate cell formation on the villi. Furthermore, HER2^{V777L} expression, in the context of adenomatous polyposis coli (APC) loss, further enhanced proliferation of small intestinal crypts. These data provide the first insight into the role of HER2^{V777L} expression on intestinal epithelial homeostasis and stem cell populations.

Results

HER2^{V777L} Expression Driven by Lgr5-CreERT2 Enhances Crypt Depth and Villus Length

HER2 transgenic (Tg) mice expressing the Lox-STOP-Lox HER2^{V777L} transgene (HER2^{V777L} Tg) were generated using transcription activator-like effector nucleases (TALEN)–based gene editing (Figure 1A). The HER2^{V777L} mutation is a constitutively activated mutation that has been identified in human colorectal cancer patients.[5] Because CRC arises from intestinal stem cells, we utilized the Lgr5-CreERT2 mouse strain, which expresses Cre-recombinase in the Lgr5-positive crypt-base columnar stem cells to activate HER2^{V777L} expression.[10,11]

To assess the role of HER2^{V777L} expression on the intestinal epithelium, 2-month-old Lgr5-Cre; HER2^{V777L} Tg and littermate control mice were treated with tamoxifen for 3 consecutive days and sacrificed 10 days after the last injection (Figure 1B). Increased phosphorylation of HER2 and increased total HER2 were observed by western blotting in jejunal and colonic tissue lysates from Lgr5-Cre; HER2^{V777L} Tg mice relative to littermate control mice treated with tamoxifen (Figure 1C). The Lgr5-CreERT2 mouse is known to give mosaic or variegated Cre expression in the intestine[11] and we found that approximately 60% of small intestinal crypts and villi had strong HER2^{V777L} expression. HER2^{V777L} transgene expression resulted in hypertrophic crypt formation in the proximal small intestine, distal small intestine, proximal colon, and distal colon relative to littermate control mice (Figure 1D–G). In the mucosal folds of the proximal colon, HER2^{V777L} expression also triggered remodeling of the epithelium with a transformation of flat, crypt cuffs (in control mice) into finger-like projections resembling villi (Figure 1F). This phenotype was less pronounced in the distal colon of HER2^{V777L} mice, where expression of HER2 showed greater variegation compared with proximal intestinal areas (Figure 1G). HER2^{V777L} nonexpressing crypts or villi in the small intestine and colon were morphologically identical to littermate control mice. The observed hypertrophic phenotype in the intestine was also illustrated by enhanced crypt depth in Lgr5-Cre; HER2^{V777L} Tg mice in the proximal small intestine, distal small intestine, proximal colon, and distal colon (Figure 1H). HER2^{V777L} expression also resulted in an expanded zone of proliferating cells as measured by Ki-67 staining in all regions of the intestine (Figure 1I). Proximal small intestinal crypts of

Most current article

Lgr5-Cre; HER2^{V777L} Tg mice also showed increased phosphorylated mitogen-activated protein kinase (p-MAPK), a known downstream signaling protein of HER2, via immunofluorescence staining (Figure 1L). Last, HER2^{V777L} expression was also associated with enhanced villus length in the proximal and distal small intestine
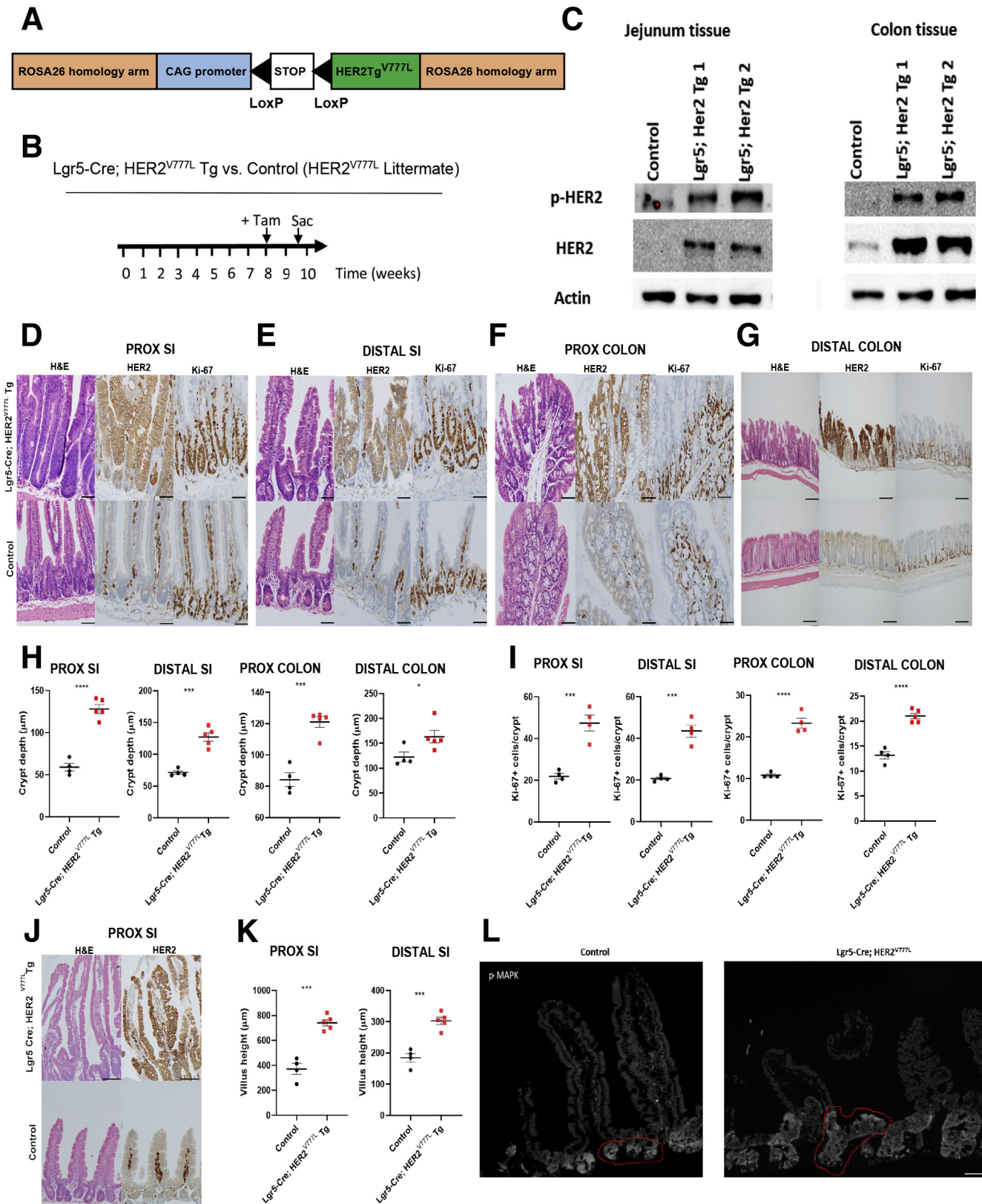
relative to control mice (Figure 1*J* and *K*). These findings demonstrate that HER2^{V777L} expression resulted in morphologic alterations of both proliferative and differentiated compartments of the intestine.

HER2^{V777L} Expression Increases Intestinal Stem Cell Markers and Expression of Wnt Target Genes in the Proximal Small Intestine

Due to the enhanced crypt depth in Lgr5-Cre; HER2^{V777L} Tg mice, we next examined whether expression of intestinal stem cell markers in the proximal jejunum were altered using quantitative reverse-transcription polymerase chain reaction (qRT-PCR). Messenger RNA (mRNA) expression of the stem cell markers, Bmi1, Olfm4, and Lrig1 were increased in Lgr5-Cre; HER2^{V777L} Tg mice relative to control mice, whereas expression of Lgr5 did not significantly change in these same mice (Figure 2*A*). One possible explanation for this difference in Lgr5 compared with other stem cell markers is that the Lgr5 Cre-recombinase allele results in knock-out of 1 copy of the Lgr5 gene. Other Wnt target genes such as Axin2, Cd44, and c-Myc showed elevated mRNA expression in Lgr5-Cre; HER2^{V777L} Tg mice (Figure 2*B*). These qRT-PCR measurements represent a population average across the HER2^{V777L} expressing and nonexpressing regions of the epithelium. Taken together, our data suggest that HER2^{V777L} expression enhances Wnt signaling and markers of intestinal stem cells that may provide an explanation for the enhanced crypt depth observed in these mice.

HER2^{V777L} Expression Promotes Enhanced Expression of Secretory and Absorptive Markers in the Proximal Small Intestine

Given the differences observed in the stem cell population of Lgr5-Cre; HER2^{V777L} Tg mice, we next examined expression of markers of differentiated epithelial lineages. We found evidence that mRNA markers for differentiation of 4 major cell types were altered in Lgr5-Cre; HER2^{V777L} Tg mice. A Paneth cell marker, lysozyme, and goblet cell markers, Muc2 and Tff3, showed increased expression in Lgr5-Cre; HER2^{V777L} Tg mice, relative to littermate control mice, whereas expression of Defcr5 (another Paneth cell marker) remained unchanged. Additionally, expression of markers for enteroendocrine cell lineages, chromogranin A

and neurog3, was also enhanced in Lgr5-Cre; HER2^{V777L} Tg mice (Figure 2C). Interestingly, the absorptive cell markers, Alpi and Fabp1, were increased in Lgr5-Cre; HER2^{V777L} Tg mice (Figure 2*D*). The increase in secretory and absorptive markers was accompanied by increased expression of the transcription factors Atoh1, Hes1, and Gfi1, suggesting that HER2^{V777L} promotes intestinal differentiation (Figure 2*E*). Overall, our data suggest that HER2^{V777L} expression in the proximal small intestine promotes a concomitant secretory cell hyperplasia as well as enhanced expression of absorptive markers, which is consistent with the increased villus height observed in our Tg mouse model.

In contrast to the increased stem cell markers observed in the small intestine, significant changes in Bmi1 or Olfm4 expression were not observed in the colon tissue of Lgr5-Cre; HER2^{V777L} Tg mice. This result is largely due to the absence of Bmi1 or Olfm4 expression in the colon (Figure 2*F*). However, decreased expression of the stem cell markers Lrig1 and Lgr5 were observed, suggesting that HER2^{V777L} expression limits expansion of stem cell populations in the colon. In addition, HER2^{V777L} expression also resulted in decreased expression of Wnt target genes, Axin2, Cd44, and c-Myc, which contrasted the enhanced expression of Wnt target genes observed in the small intestine (Figure 2*G*). Expression of the secretory cell marker, Muc2 was also decreased in Lgr5-Cre; HER2^{V777L} colon organoids, suggesting that HER2^{V777L} expression in the colon alters differentiation of secretory cells (Figure 2*H*). Last, expression of the absorptive marker, Alpi, was increased in Lgr5-Cre; HER2^{V777L} colon tissue, whereas expression of the transcription factors Hes1 and Gfi1 were decreased (Figure 2*I* and *J*, respectively). As a result, HER2^{V777L} expression in the colon resulted in decreased expression of stem cell markers and altered differentiation, which contrasted the phenotype observed in the small intestine. Additionally, the expression changes in stem cell and secretory cell markers induced by HER2^{V777L} in the colon also may reflect spatial and functional differences between the small intestine and colon.

HER2^{V777L} Expression Increases Absorptive Cells and Promotes Intermediate Cell Formation in the Proximal Small Intestine

We next assessed relative cellular abundance of intestinal epithelial stem, Paneth, goblet, and absorptive cells

Figure 1. (*See previous page*). **HER2^{V777L} expression confers hypertrophic crypt formation in vivo.** (*A*) Schematic for design of HER2^{V777L} Tg mouse. (*B*) Lgr5-Cre; HER2^{V777L} and HER2^{V777L} littermate mice were treated with tamoxifen at 8 weeks of age for 3 consecutive days and sacrificed 10 days after the last injection. (*C*) Western blotting from jejunum and colon tissues for phospho-HER2 and total HER2 from tamoxifen-treated mice. (*D–G*) HE, HER2, and Ki-67 images of proximal small intestine, distal small intestine, proximal colon, and distal colon tissue sections from Lgr5-Cre; HER2^{V777L} Tg and littermate control mice, respectively. Scale bars are 50 μm. (*H*) Quantification of crypt depth for proximal small intestine, distal small intestine, proximal colon, and distal colon as measured in micrometers. Eighty HER2 expressing crypts per mouse were measured and n $\geq$ 4 per group. (*I*) Quantification of Ki-67 positive cells per crypt and n $\geq$ 4 per group (*J*) HE and HER2 staining of Lgr5-Cre; HER2^{V777L} Tg and littermate control villi. (*K*) Quantification of villus length for proximal and distal small intestine. Eighty HER2 expressing villi per mouse were measured and n = 3 per group. Data are plotted as means, 1 dot represents 1 mouse, and mean $\pm$ SEM are reported. **$P < .01$, ***$P < .001$, and ****$P < .0001$ as calculated by the Student *t* test. (*L*) Representative grayscale images of phosphorylated MAPK (p-MAPK) immunofluorescence staining of the proximal small intestine of littermate control and Lgr5-Cre; HER2^{V777L} mice. Scale bars are 100 μm.
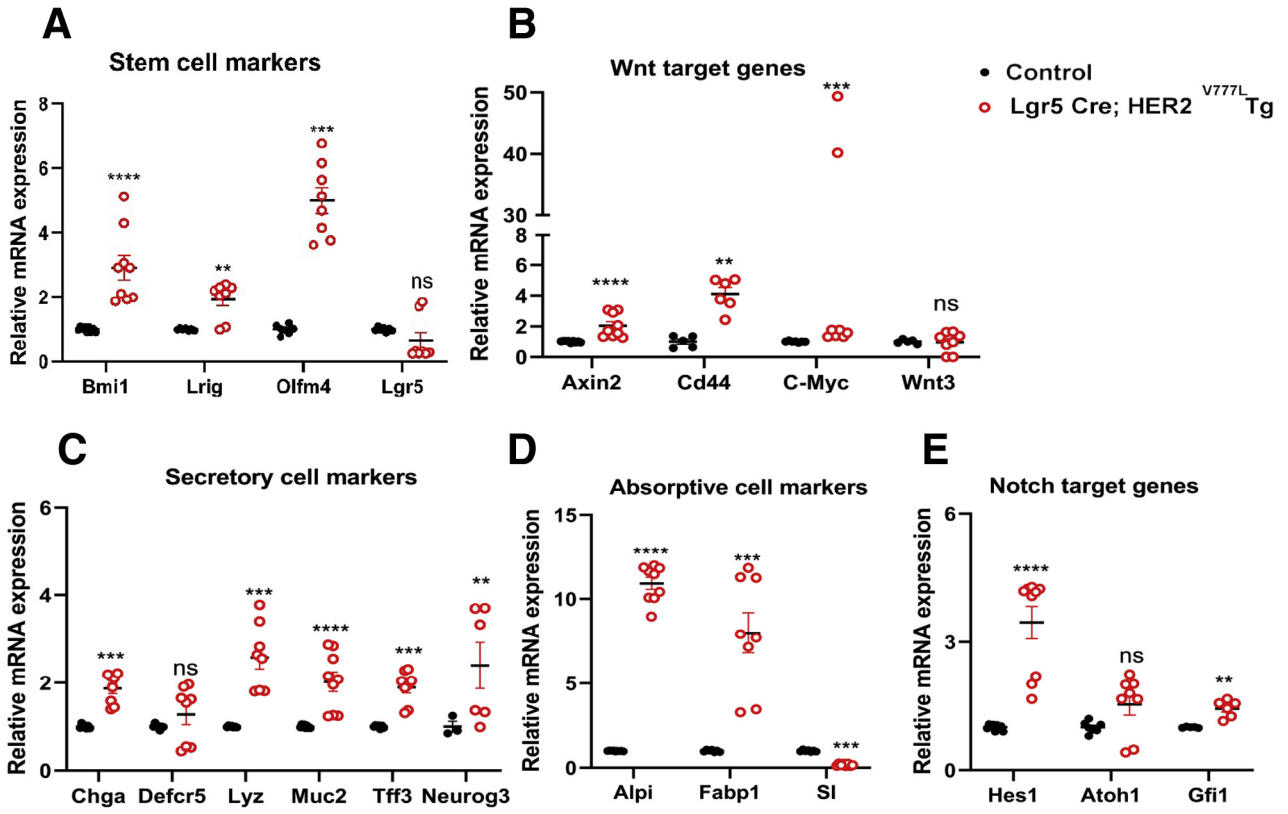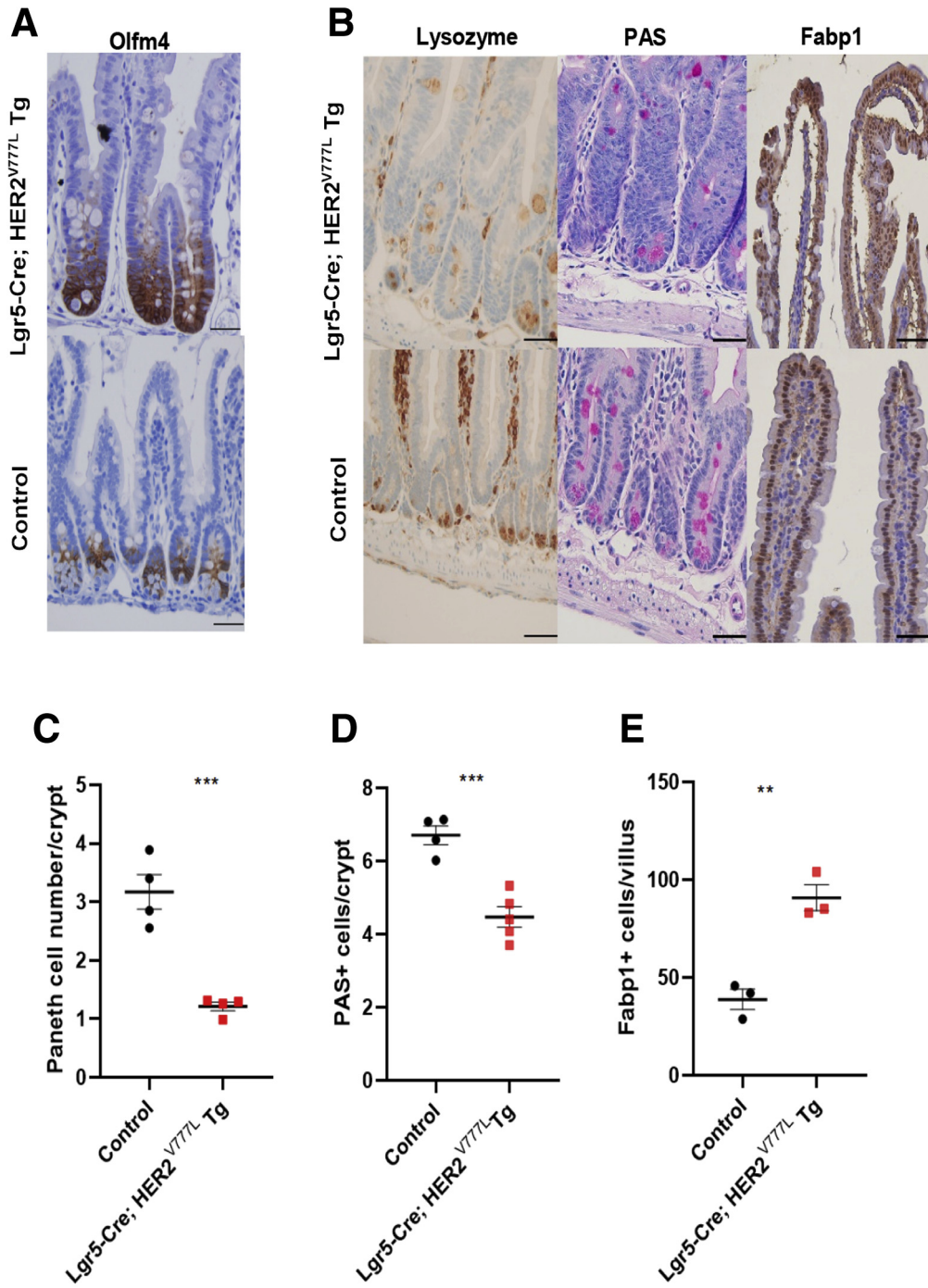
Jejunum tissue
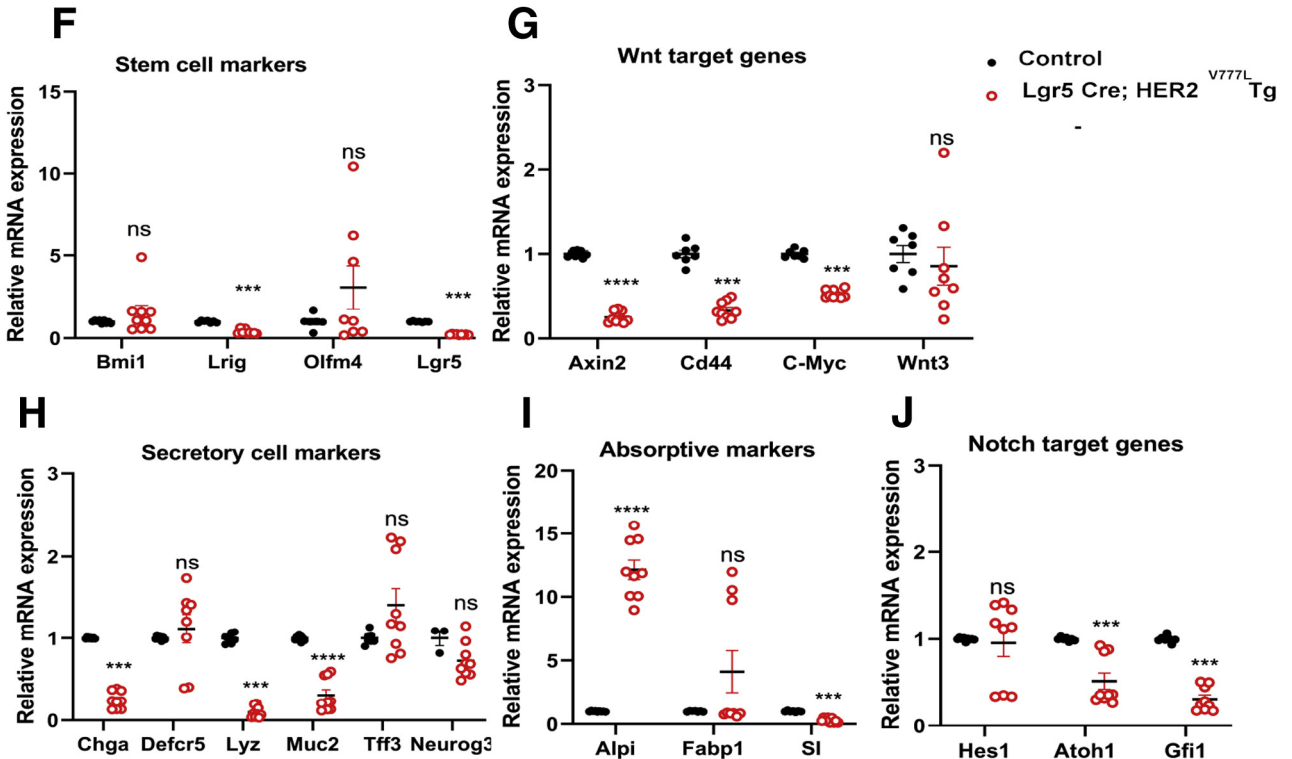
Figure 3. HER2^{V777L} expression decreases Paneth cell number per crypt. (A) Immunohistochemistry staining for Olfm4 in the proximal small intestine of Lgr5-Cre; HER2^{V777L} Tg and littermate control mice. Representative images are shown. Scale bars are 50 μm. (B) Immunohistochemistry staining for lysozyme, periodic acid-Schiff (PAS), and Fabp1 of Lgr5-Cre; HER2^{V777L} Tg and littermate control mice. Scale bars are 50 μm. (C) Quantification of Paneth cell number per crypt, (D) PAS-positive cells per crypt, and (E) Fabp1-positive cells per crypt. Eighty crypts were measured and n $\geq$ 3 per group.

in the proximal jejunum using immunohistochemistry. Expression of Olfm4, a crypt-based columnar marker, was expanded throughout Lgr5; Cre-HER2^{V777L} Tg crypts, suggesting that Olfm4 expressing stem cells were expanded in our mouse model (Figure 3A). Paneth cells at crypt bases were decreased relative to littermate control

Figure 2. (*See previous page*). **HER2^{V777L} expression increases intestinal stem cell populations and expression of absorptive markers.** Small intestinal tissue from Lgr5-Cre; HER2^{V777L} Tg and littermate control mice were examined for the expression of (A) stem cell markers, (B) Wnt target genes, (C) secretory cell markers, (D) absorptive markers, and (E) Notch target genes via qRT-PCR. Colon tissue from Lgr5-Cre; HER2^{V777L} Tg and littermate control mice were examined for the expression of (F) stem cell markers, (G) Wnt target genes, (H) secretory cell markers, (I) absorptive markers, and (J) Notch target genes via qRT-PCR. 18s ribosomal RNA was used as a reference gene. n = 3 mice per group, with 2 or 3 technical replicates performed for each mice. Data are plotted as mean $\pm$ SEM, 1 dot represents 1 data point. *$P < .05$, **$P < .01$, ***$P < .001$, and ****$P < .0001$ as calculated by the Mann-Whitney U test.
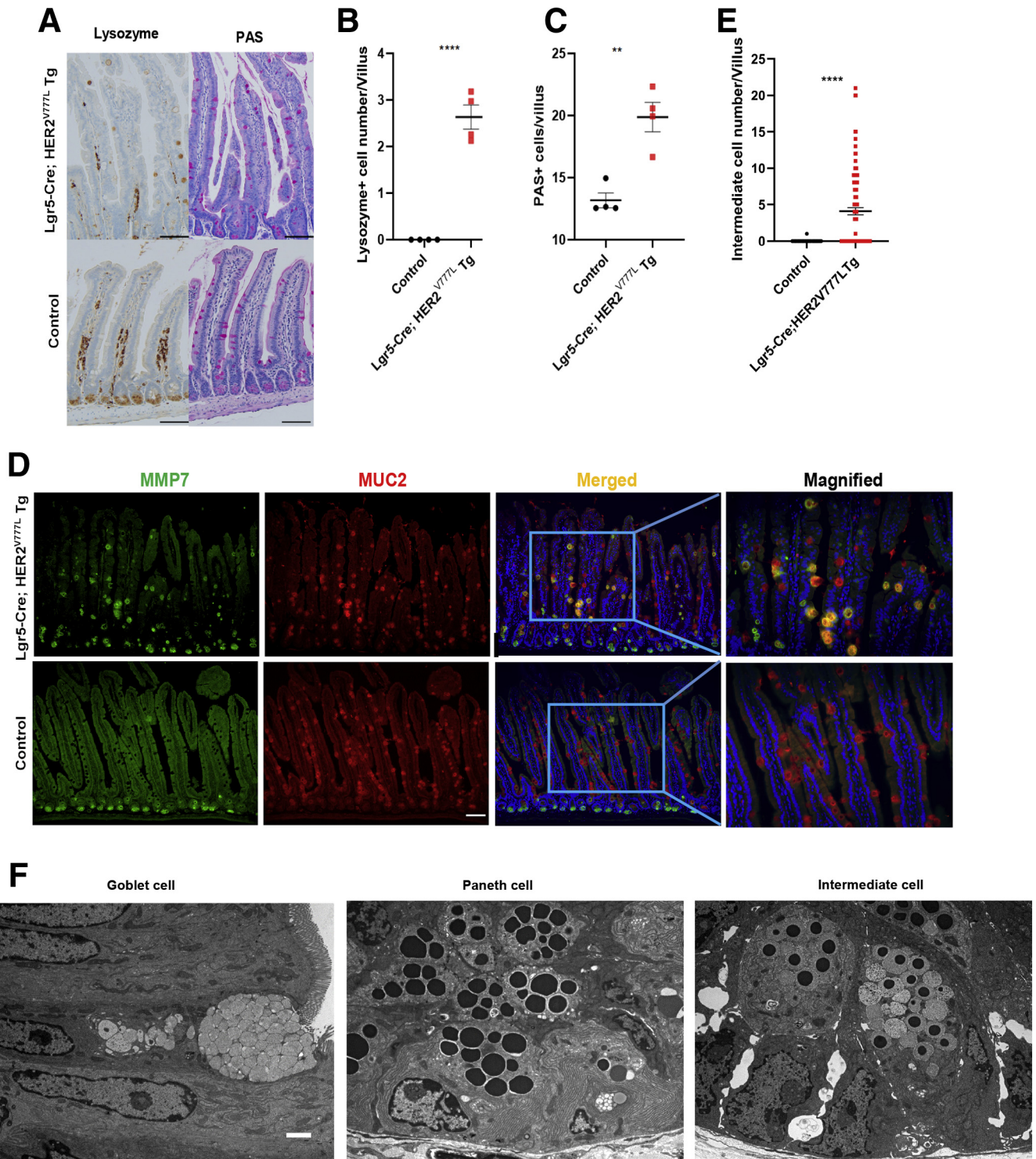
Figure 4. HER2^{V777L} **expression increases intermediate cells per villi in the small intestine.** (*A*) Immunohistochemistry staining for lysozyme and PAS on intestinal villi. Scale bars are 100 μm. (*B*) Quantification of Paneth cell number per villus and (*C*) quantification of PAS-positive cells per villus. Eighty intestinal villi were measured; n = 4 per group. (*D*) Representative immunofluorescence staining of the proximal small intestine of Lgr5-Cre; HER2^{V777L} Tg and littermate control mice using MUC2 (red) and MMP7 (green) and merged images (with DAPI, blue). Yellow-colored cells indicate presence of intermediate cells with green and red colors merged. Scale bars are 100 μm. (*E*) Quantification of intermediate cells for the proximal small intestine. More than 50 villi were counted per mouse and n = 2 per group. (*F*) Transmission electron microscopy (TEM) representative images of goblet cells on the villi, Paneth cell at the base of the crypt, and intermediate cells near the crypt from Villin-Cre; HER2^{V777L} Tg mice. Scale bars are 2 μm.

mice, as assessed by lysozyme and periodic-acid Schiff staining (Figure 3B–D). Lgr5-Cre; HER2^{V777L} Tg mice also possessed increased numbers of enterocytes as assessed by Fabp1 staining (Figure 3B and E), which correlated with the mRNA expression data shown in Figure 2D.
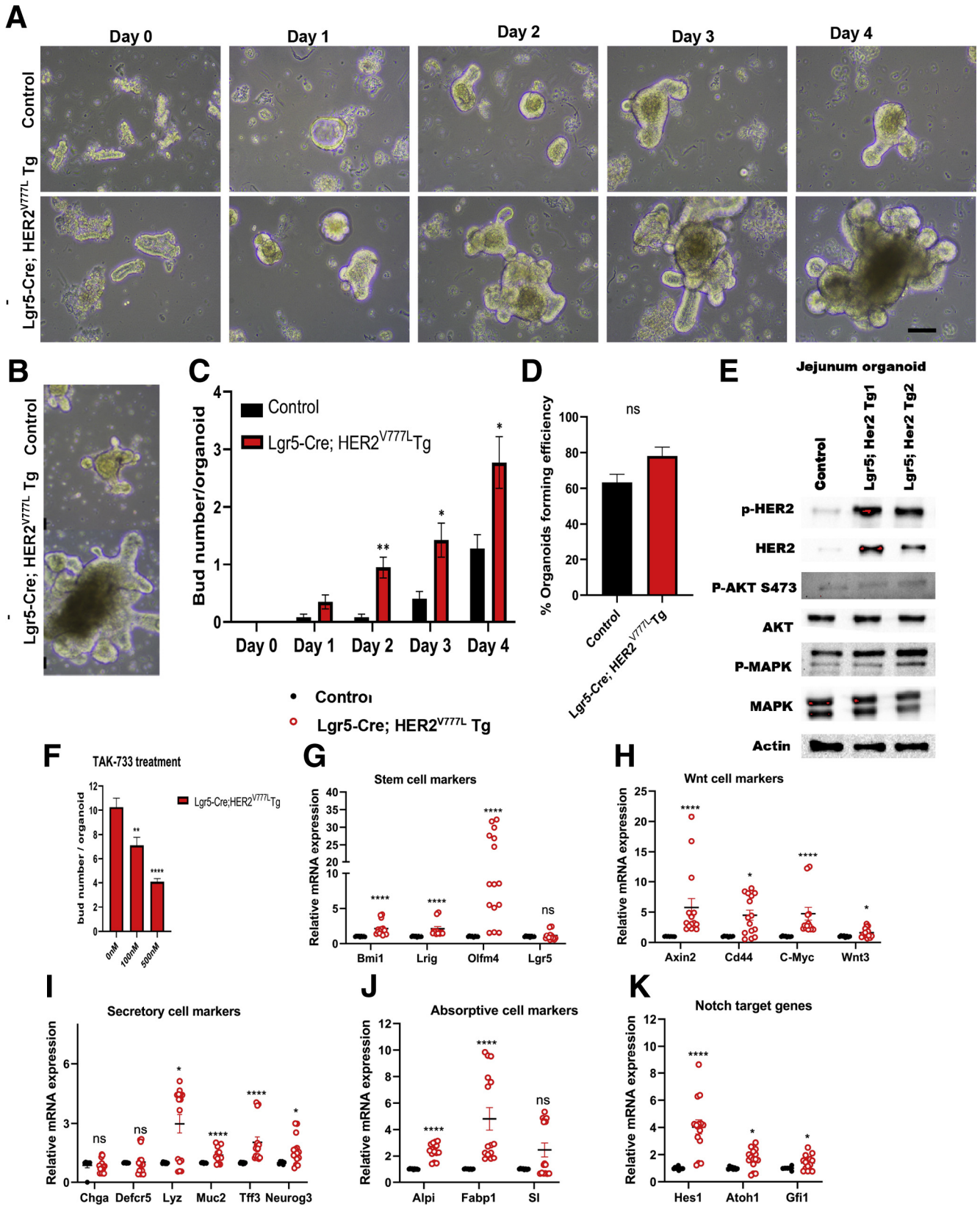
Interestingly, although Paneth cells were reduced per crypt, the number of lysozyme positive cells was enhanced along villi (Figure 4A and B). Additionally, goblet cell number was increased in Lgr5-Cre; HER2^{V777L} Tg villi relative to littermate control mice (Figure 4A and C). Morphologically, the lysozyme positive cells observed on the villus showed dual staining for goblet and Paneth markers (MMP7 and MUC2), indicating that these cells may be intermediate cells (Figure 4D and E).[12,13] Furthermore, transmission electron microscopy of jejunum-derived intestinal crypts also identified intermediate cells, which are characterized by the presence of apical mucin granules that each contain a single electron dense foci within them (Figure 4F; last panel). These granules were distinct in morphology from goblet or Paneth cells in control mice (Figure 4F; first 2 panels). Overall, we determined that HER2^{V777L} expression promotes intermediate cell formation on intestinal villi.

HER2^{V777L} Expression In Vitro Confers Enhanced Small Intestinal Organoid Budding and Increased Expression of Stem Cell Markers

Next, to determine whether the enhanced growth phenotype observed in vivo is epithelial cell intrinsic or cell extrinsic, we utilized primary small intestinal epithelial organoid cultures. We generated organoids from the proximal jejunum of Lgr5-Cre; HER2^{V777L} Tg mice, confirmed their HER2^{V777L} expression, and observed changes in morphology. Lgr5-Cre; HER2^{V777L} Tg organoids possessed increased number of buds after growth in EGF, Noggin, and R-spondin media over a 4-day period relative to littermate control organoids, which correlated with the enhanced crypt size observed in vivo (Figure 5A–C). Organoid forming efficiency was not significantly enhanced by HER2^{V777L} expression, suggesting that HER2^{V777L} expression increases budding after initial formation of organoids (Figure 5D). Last, to determine whether the enhanced growth phenotype was due to enhanced downstream signaling, immunoblotting of small intestine organoids derived from tamoxifen-treated mice was performed. HER2^{V777L} expression resulted in a modest increase in MAPK phosphorylation and did not change Akt signaling (Figure 5E). Treatment of the intestinal organoid cultures with a MEK inhibitor, TAK-733, reduced organoid budding, supporting a partial role for the MEK-MAPK pathway in this phenotype. However, we found that higher doses of this inhibitor decreased organoid

viability, likely due to the fact that the MEK-MAPK pathway is involved in many essential signal pathways (Figure 5F). Last, owing to the enhanced budding phenotype observed, we also sought to determine whether expression of stem cell and secretory cell markers were enhanced in our intestinal organoid model. Similar to the trends observed in small intestine tissue, HER2^{V777L} expression resulted in increased expression of the stem cell markers, Bmi1, Lrig1, and Olfm4 but not Lgr5 (Figure 5G). The increase in stem cell markers was also accompanied by an increase in Wnt target genes, which suggests that enhanced Wnt signaling may play a role in the expansion of stem cells observed (Figure 5H). Last, HER2^{V777L} expression also conferred increased expression of all secretory cell types examined as well as increased expression of absorptive markers and Notch target genes, which correlated with the trends observed in the small intestinal tissue (Figure 5I–K). As a result, the stem cell and absorptive cell phenotypes observed in the small intestine in vivo can be recapitulated in our intestinal organoid culture model, supporting that the in vivo phenotypes are epithelial cell autonomous.

HER2^{V777L} Expression in Colon Organoids Does Not Alter Organoid Morphology and Decreases Expression of Stem Cell Markers

Last, owing to the distinct morphological changes observed in the small intestine, we also sought to examine the effect of HER2^{V777L} expression on proximal colon organoids derived from Lgr5-Cre; HER2^{V777L} Tg mice. HER2^{V777L} expression did not result in changes in colon organoid morphology, perhaps owing to the highly proliferative Wnt, R-spondin, and Noggin media used to culture the colon organoids (Figure 6A). An increase in total HER2^{V777L} expression was confirmed by western blotting in the Lgr5-Cre; HER2^{V777L} Tg colon organoids derived from tamoxifen-treated mice; however, significant changes in MAPK or Akt phosphorylation were not observed (Figure 6B). Last, we utilized quantitative PCR analysis to assess changes in the expression levels of stem cell, secretory cell, and absorptive marker genes in proximal colon-derived organoid cultures. The expression levels of the stem cell markers Bmi1 and Lgr5 and Wnt-target genes Cd44 and c-Myc were decreased in colon organoids derived from tamoxifen-treated Lgr5-Cre; HER2^{V777L} Tg mice relative to littermate control mice (Figure 6C and D). In

Figure 5. (*See previous page*). **Expression of HER2^{V777L} in small intestinal organoids confers enhanced budding and increased expression of stem cell and absorptive markers.** (*A*) Representative image of small intestinal organoids generated from the jejunum of Lgr5-Cre; HER2^{V777L} Tg and control mice grown over a 4-day period in EGF, noggin, and R-spondin media. (*B*) Higher magnification image of intestinal organoid cultures are shown. Scale bars are 500 μm. (*C*) Quantification of the average number of buds per organoid. Three technical replicates are shown and n = 3 mice per group for Lgr5-Cre; HER2^{V777L} Tg organoids. (*D*) Quantification of organoid forming efficiency in intestinal organoids derived from the jejunum of Lgr5-Cre; HER2^{V777L} Tg and littermate control mice after 3 days in culture. (*E*) Western blot for phospho-HER2 and total HER2 from indicated mice. (*F*) Treatment of Lgr5-Cre; HER2^{V777L} Tg–derived jejunum organoids with TAK-733 for 4 days. Cell viability was >80% at 100 nM and approximately 50% at 500 nM TAK-733. Small intestinal organoids from Lgr5-Cre; HER2^{V777L} Tg and littermate control mice were examined for the expression of (*G*) stem cell markers, (*H*) Wnt target genes, (*I*) secretory cell markers, (*J*) absorptive cell markers and (*K*) Notch target genes via qRT-PCR. 18s ribosomal RNA was used as a reference gene. n ≥ 3 per group. Technical duplicate or triplicate for each mice. Data are plotted as mean ± SEM, 1 dot represents 1 data point. *P < .05, **P < .01, ***P < .001, and ****P < .0001 as calculated by the Mann-Whitney U test.
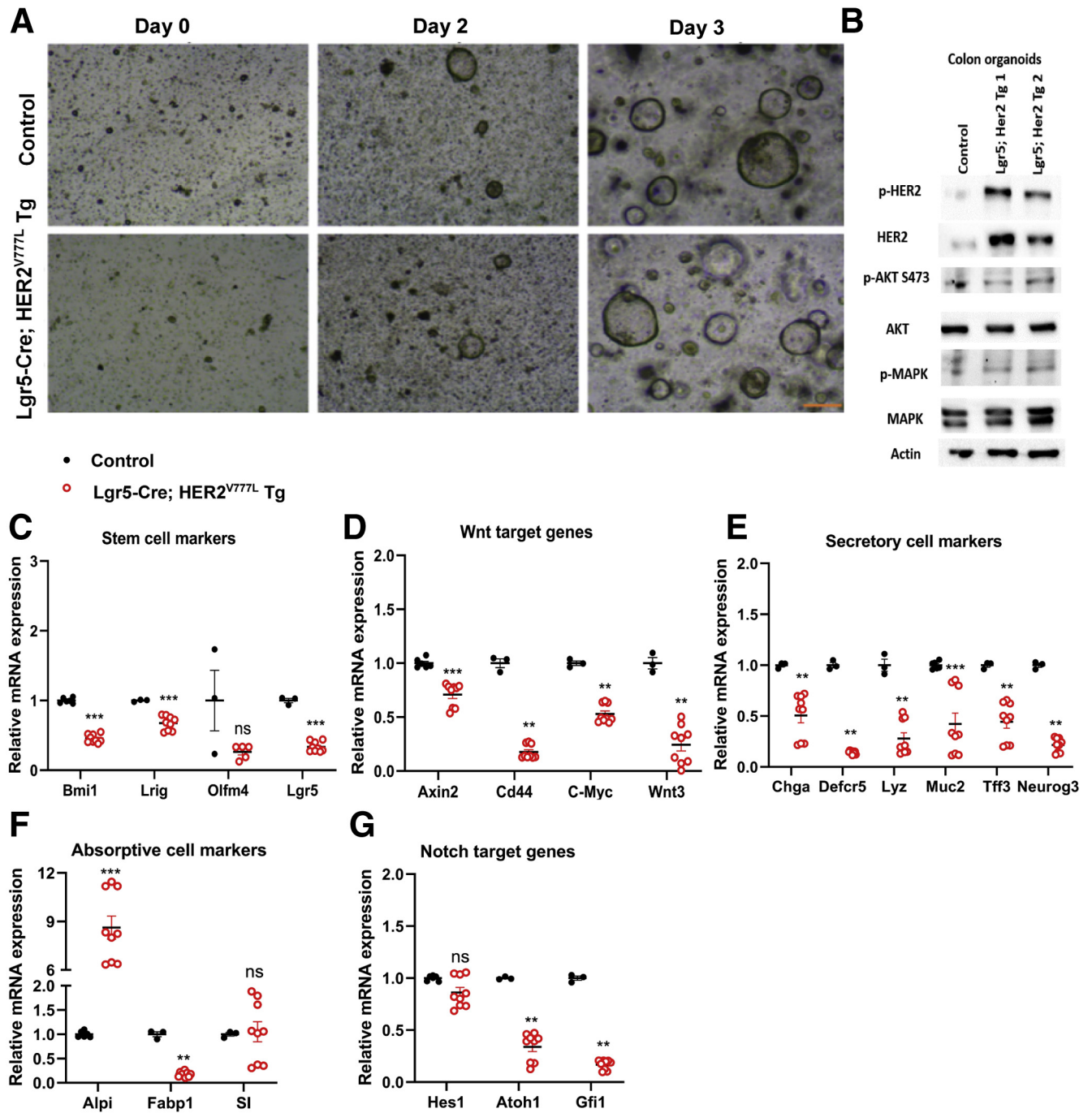
Figure 6. Colon organoids from Lgr5-Cre; HER2^{V777L} Tg and littermate control mice. (*A*) Representative image of colon organoids generated from Lgr5-Cre; HER2^{V777L} Tg and littermate control mice grown in 50% L-WRN conditioned media. Scale bars are 200 μm. (*B*) Western blot for phospho-HER2 and total HER2 from indicated mice treated with tamoxifen in vivo. Colon organoids from Lgr5-Cre; HER2^{V777L} Tg and littermate control mice were examined for the expression of (*C*) stem cell markers, (*D*) Wnt-target genes, (*E*) secretory cell markers, (*F*) absorptive cell markers, and (*G*) Notch target genes via qRT-PCR. 18s ribosomal RNA was used as a reference gene. n = 3 mice per group, with 2 or 3 technical replicates performed for each mice. Data are plotted as mean ± SEM, 1 dot represents 1 data point. *$P < .05$, **$P < .01$, ***$P < .001$, and ****$P < .0001$ as calculated by the Mann-Whitney *U* test.

addition, significant changes in the expression of goblet cell and enteroendocrine cell markers Tff3 and ChgA were observed in colon organoids derived from Lgr5-Cre; HER2^{V777L} mice (Figure 6*E*). In contrast, increased expression of Alpi, an absorptive marker, was also observed in Lgr5-Cre; HER2^{V777L} organoid cultures (Figure 6*F*). The increased expression of absorptive markers observed also likely reflects the abundance of absorptive cells normally present in the colon. Overall, HER2^{V777L} expression in colon organoids did not result in expansion of the stem cell
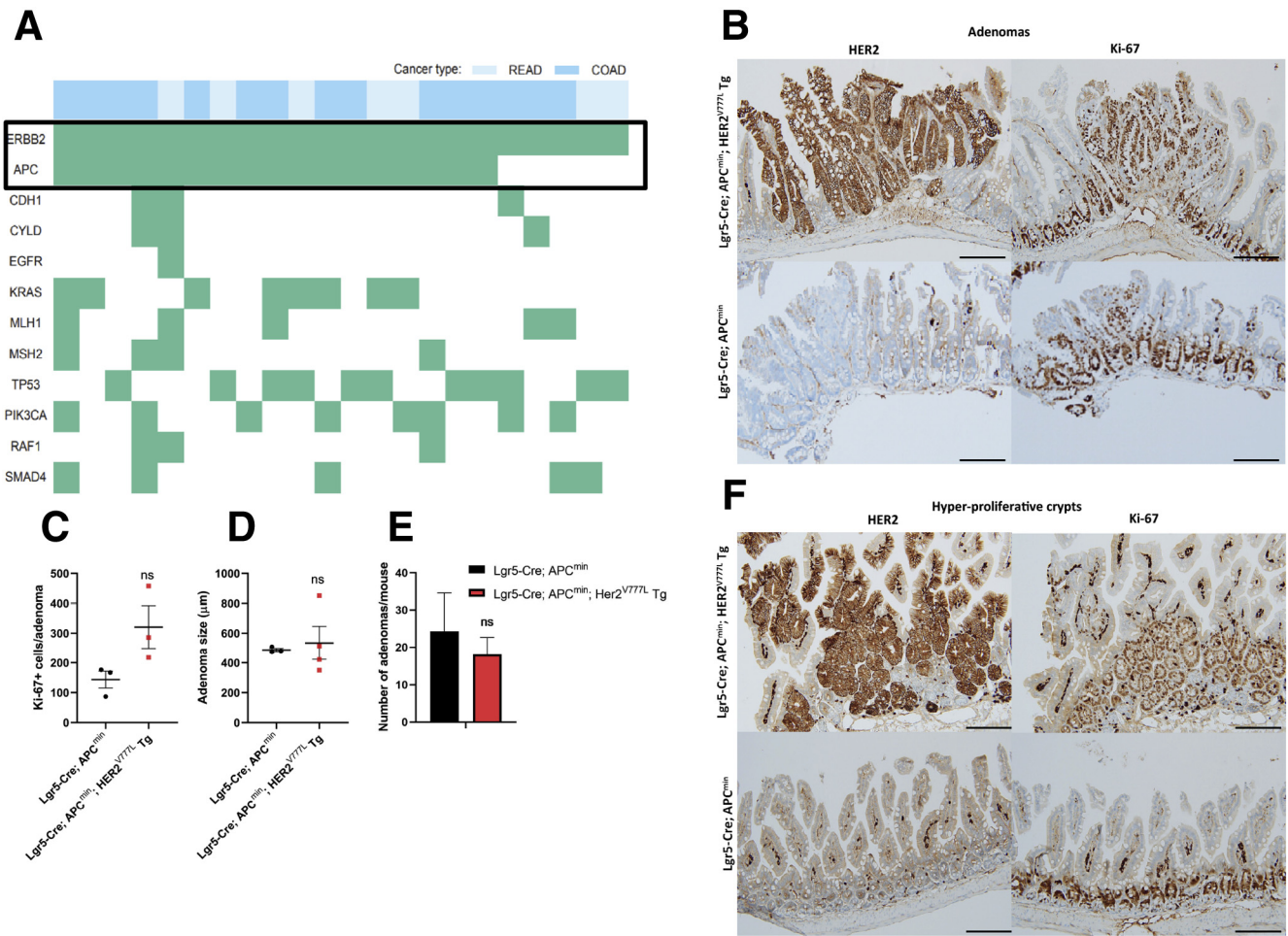
Figure 7. HER2^{V777L} expression promotes hyperproliferation in the context of APC loss. (*A*) Colon adenocarcinoma (COAD) or rectum adenocarcinoma (READ) patients were extracted from The Cancer Genome Atlas Unified Ensemble call set resulting in a total of 559 patients. All COAD (blue) and READ (light blue) patients found to have missense mutations in ERBB2 that co-occur with any other mutation type in a subset of genes are highlighted on the left. (*B*) Immunohistochemistry staining for HER2 and Ki-67 in intestinal adenomas of Lgr5-Cre; APC^{min}; HER2^{V777L} Tg and Lgr5-Cre; APC^{min} mice. Scale bars are 100 μm. (*C*) Quantification of the average number of Ki-67–positive cells per adenoma. n = 3 per group. (*D*) Average adenoma size per mouse as measured in micrometers. n $\geq$ 3 per group. (*E*) Quantification of adenoma number per mouse (proximal and distal small intestine). n = 3 per group. (*F*) Immunohistochemistry staining for HER2 and Ki-67 in hyperproliferative crypts. *Scale bars are 100 μm. No significant differences measured by t test in C–E.*

population, and distinct changes in organoid morphology were not observed as a result.

APC Loss Combined With Short-Term HER2^{V777L} Expression Generates a Hyperproliferative Phenotype in Intestinal Crypts

Next, we examined the role of co-occurring mutations on tumorigenesis using our HER2^{V777L} Tg mouse model. Colorectal cancer patients possessing HER2 missense mutations possess several co-occurring mutations in tumor suppressor genes such as APC, TP53, and oncogenes such as, KRAS and PIK3CA (Figure 7*A*).[14] Of these co-occurring mutations, HER2 and APC mutations were the most prevalent, and we sought to examine the role of both HER2 and APC mutations

on tumor progression using an APC^{min} mouse model. Lgr5-Cre; HER2^{V777L} Tg mice were crossed with heterozygous APC^{min} mice to generate Lgr5-Cre; APC^{min}; HER2^{V777L} Tg mice and these mice were treated with tamoxifen at 8 weeks of age and sacrificed 10 days after the last injection to study short-term changes induced by APC and HER2 mutations. Intestinal adenomas in Lgr5-Cre; APC^{min}; HER2^{V777L} Tg mice and Lgr5-Cre; APC^{min} control mice were also analyzed via immunohistochemistry staining. Surprisingly, HER2^{V777L} expression did not result in significant increases in the number of Ki-67–positive cells per adenoma, average adenoma size, or number per mouse (Figure 7*B*–*E*). However, Lgr5-Cre; APC^{min}; HER2^{V777L} Tg mice possessed several hyperproliferative regions characterized by proliferative

crypts that protrude toward villus tips (Figure 7F). These hyperproliferative regions were not observed in Lgr5-Cre; APC[min] control mice. Overall, we determined that HER2 and APC mutations promote a hyperproliferative environment that may promote a tumor initiating phenotype, rather than tumor progression. Co-occurring mutations in TP53 and the SMAD pathway are likely needed to observe cancerous phenotypes.

Discussion

Roughly 7% of colon cancer patients possess HER2 mutations or amplification. Previous research has identified several HER2 mutations in the kinase domain that activate downstream signaling pathways and confer enhanced growth, such as HER2[V777L].[5] Our work is the first to characterize the role of HER2[V777L] expression on the intestinal epithelium using Tg mice. We hypothesized that expression of HER2[V777L] would promote crypt hyperplasia and enhanced proliferation due to the role of HER2 and other EGFR family members on cell growth and proliferation using in vitro models.[15,16] Prior studies exploring the role of HER2 on the intestinal epithelium have determined that HER2 does promote intestinal epithelial recovery from injury, but intestinal epithelial knockout of HER2 does not alter intestinal crypt or villus morphology, proliferation, or migration, possibly because of functional overlap with HER3.[7] Similarly, additional studies on the role of HER3 determined that expression of this receptor does not alter intestinal proliferation or migration, and that these receptors instead play crucial roles during tumorigenesis.[8] The results presented using our HER2 Tg mouse model, however, illustrate for the first time, the role of an activating HER2[V777L] mutation on intestinal epithelial homeostasis and crypt-villus architecture.

Using our Tg mouse model, we determined that HER2[V777L] expression in the proximal small intestine increased crypt depth and villus length via enhanced proliferation and expansion of progenitor stem cells. In contrast, expression of HER2[V777L] in the proximal colon resulted in abnormal morphology of the mucosal folds; however, increased expression of stem cell and secretory cell markers were not observed as a result of HER2[V777L] expression. As a result, expression of HER2[V777L] has differential effects on stem cell and secretory cell populations depending on the region of the intestine, and the strongest phenotypes induced by our mouse model were observed in the small intestine. In addition, the enlarged crypt phenotype observed in our mouse model is similar to mouse models expressing the KRAS G12D mutation, wherein a similar expanded crypt phenotype is characterized by increased proliferation via enhanced MAPK signaling and increased Hes1 expression.[17] Underlying mechanisms for the hyperproliferative phenotypes observed in our Tg mouse model are likely due to enhanced activation of phosphorylated MAPK in the proximal small intestine as assessed by immunofluorescence staining and increased expression of the Notch transcription factors Hes1 and Gfi1;

however, additional studies are needed to confirm potential mechanisms. We also assessed whether the hyperproliferative phenotypes observed in vivo could be recapitulated using intestinal organoid cultures. HER2[V777L] expression in intestinal organoids conferred an increase in bud number due to an increase in stem cell markers as determined by quantitative PCR. Prior studies assessing the role of Lrig1, a negative regulator of EGFR signaling, have also determined that knockout of Lrig1 also results in an increased number of organoid buds due to increased expression of HER2 and HER3.[18]

In addition, we also determined that HER2[V777L] expression promotes intermediate cell formation on the intestinal villi. One potential mechanism for this effect is through the Rho family GTPases, Rac1 and Cdc42. HER2 is known to signal to Rac1 and Cdc42 through p120 Catenin,[19] and modulation of Rac1 or Cdc42 has been shown to alter Paneth and goblet cell differentiation.[13,20] Introduction of a dominant negative Rac1 mutant in the intestinal epithelium resulted in increased intermediate cells, decreased mature goblet cells, and a less prominent reduction in Paneth cells, whereas introduction of constitutively active Rac1 mutant caused precocious differentiation of Paneth cells and enterocytes.[13] Likewise, knockout of Cdc42 also increased intermediate cell formation.[20] Notch blockade has also been shown to increase intermediate cell formation[21]; however, expression of the HER2[V777L] transgene resulted in increased expression of the Notch transcription factor, Hes1, in the jejunum, suggesting that Notch signaling inhibition is not the cause of increased intermediate cell formation observed in HER2[V777L] Tg mice.

Last, our studies to examine the role of HER2 and APC mutations on tumorigenesis illustrated that HER2[V777L] expression lead to a hyperproliferative phenotype in Lgr5-Cre; APC[min]; HER2[V777L] Tg mice. Our experiments focus on acute changes induced by HER2[V777L] expression and our work does not attempt to explore how HER2[V777L] expression could be impacting tumor progression over a longer time period, and thus we did not observe an increase in the number or size of intestinal adenomas in Lgr5-Cre; APC[min]; HER2[V777L] Tg mice in the acute time frame. Our results complement longer-term studies on the role of EGFR family members on tumorigenesis, which showed that genetic inactivation of EGFR or HER3 significantly decreases tumor formation in APC[min] mouse models, suggesting that these receptors play important roles in tumor formation.[6,8] Additionally, expression of our HER2[V777L] transgene might require additional mutations, such as in p53 and SMAD genes, for progression of adenomas to carcinomas.

In summary, we determined that HER2[V777L] expression resulted in hypertrophic crypt formation, expanded stem cell populations, and increased intermediate cells in the proximal small intestine. Expression of both HER2 and APC mutations resulted in enhanced proliferation of the crypt compartment. This work is the first to generate a Tg mouse model for HER2 activating mutations and characterizes the effect of HER2[V777L] on the intestinal epithelium. Our results suggest an epithelial intrinsic role of

$HER2^{V777L}$ on hyperproliferation and enhanced intestinal stem cell populations driven by activation of downstream signaling pathways.

Materials and Methods

Mice

Generation of Tg Mice Expressing $HER2^{V777L}$ in the Intestinal Epithelium.
$HER2^{V777L}$ Tg were generated using TALEN-based genome editing. ROSA26 specific TALENs were designed using the ZiFit targeter.[22] The TALEN kit used for TALEN assembly was a gift from Keith Joung (Addgene kit # 1000000017; Addgene, Watertown, MA). DNA fragments encoding ROSA TALEN repeat arrays were cloned into plasmid pJDS71. ROSA TALENs plasmids were linearized for in vitro transcription with EcoRI and TALENs RNA was synthesized using the mMessage mMachine T7 Ultra kit (Ambion, Austin, TX) and purified with Megaclear columns (Ambion).

The cassette of interest was synthesized (Genscript, Piscataway, NJ) and introduced into the mouse genome via pronuclear injection of in vitro transcribed TALENs RNA and ROSA donor DNA. Founders with correctly targeting mutant alleles are identified using long PCR with ROSA specific oligos outside of the homology arms. Founders were bred to WT to generate heterozygous F1 offspring. Analysis of F1 offspring via long PCR confirms germline transmission of the correctly targeted allele. Primers for genotyping heterozygous offspring are the following:

ROSA-green-WT-F1: 5′ GTT ATC AGT AAG GGA GCT GCA GTG GAG TAG 3′

ROSA-green-WT-R1: 5′ CCG AAA ATC TGT GGG AAG TCT TGT CCC TCC 3′

CAG-R2: 5′ CTC CAC CCA TTG ACG TCA ATG GAA AGT CCC 3′

Lgr5-Cre ERT2 and Villin-Cre ERT2 Mice.
Lgr5-EGFP-Ires-CreERT2 mice were purchased from the Jackson Laboratory [Bar Harbor, ME; B6.129P2-Lgr5tm1(cre/ERT2) Cle/J; 008875] and Villin-Cre ERT2 mice were a gift from Blair Madison.[23] APC^{min} mice were also purchased from the Jackson Laboratory (C57BL/6J-ApcMin/J; 002020). All animal work was approved by the Washington University School of Medicine Animal Studies Committee.

Induction of Recombination

Expression of the transgene was driven by Cre-recombination of the lox-stop-lox sites. We crossed $HER2^{V777L}$ Tg mice to Lgr5-EGFP-IRES-CreERT2 or Villin-CreERT2 mice to activate HER2 expression in intestinal stem cells or the intestinal epithelial cells, respectively. To study the contribution of APC loss on the intestinal epithelium, Lgr5-Cre; $HER2^{V777L}$ Tg mice were crossed with heterozygous APC^{min} mice to generate Lgr5-Cre; APC^{min}; $HER2^{V777L}$ Tg mice.

For CreERT2-mediated recombination, 8-week-old to 5-month-old mice were injected intraperitoneally with tamoxifen (2 mg/injection; Sigma-Aldrich, St. Louis, MO) dissolved in corn oil for 3 consecutive days and sacrificed 10 days after the last tamoxifen injection. The 10-day time

point was chosen for 2 reasons. First, we wanted to allow adequate time for transit of cells from the crypt base to the tips of the villus. Second, we previously treated Villin-CreERT2; $HER2^{V777L}$ Tg mice with tamoxifen and monitored them for 1 month, but the mice died from either intestinal blockage or malabsorption caused by the marked villus hypertrophy, which constricted the intestinal lumen. Therefore, to avoid mouse deaths, a short-term time point posttamoxifen induced Cre/lox recombination was chosen. Lgr5-Cre; $HER2^{V777L}$ Tg mice showed variegated expression of the HER2 transgene with 60% of the intestinal crypts and villi having strong HER2 expression. Quantification of crypt depth and villus height was measured on HER2-expressing regions.

Immunohistochemistry of Paraffin-Embedded Sections

The proximal small intestine, distal small intestine, and colon were embedded in 2% agar, paraffin embedded, and 5-μm sections were prepared (Digestive Diseases Research Core, Washington University School of Medicine). For histology, unstained slides were stained for the indicated antibodies via immunohistochemistry (Department of Immunology and Pathology, Washington University School of Medicine). Immunohistochemistry was performed by a standard protocol on Ventana automated stainer (Ventana Medical Systems, Tucson, AZ). Antigen retrieval was performed for HER2/neu (rabbit monoclonal, clone 4B5) (Ventana Medical Systems) with CC1 buffer (Cell Conditioning 1; EDTA-based buffer pH 8.0; Ventana Medical Systems), for KI-67 2 ug/mL (rabbit monoclonal, clone 30-9; Ventana Medical Systems) with CC1 buffer (Cell Conditioning 1; EDTA-based buffer pH 8.0, Ventana Medical Systems) for lysozyme (rabbit polyclonal) (Cell Marque, Rocklin, CA) with CC1 buffer (Cell Conditioning 1; EDTA-based buffer pH 8.0; Ventana Medical Systems).

Biotin-free multimer technology system, based on direct linkers between peroxidase and secondary antibodies (ultraView Universal DAB Detection Kit; Ventana Medical Systems) were used as detection kit.

Immunofluorescence of Paraffin-Embedded Sections

Slides were de-paraffinized and subjected to heat-induced antigen retrieval in Trilogy (MilliporeSigma, Burlington, MA) solution for 20 minutes. Slides were blocked in phosphate-buffered saline containing 1% bovine serum albumin, 5% goat serum, and 0.1% Triton-X 100 for 1 hour at room temperature, and then treated with primary antibodies at desired dilutions for 16 hours at 4°C. Slides were then washed 3 times in phosphate-buffered saline and incubated with secondary antibodies conjugated with fluorophores (Thermo Fisher Scientific, Waltham, MA) for 1 hour at room temperature.[24] Primary antibodies used in the study include rabbit MUC2 (Santa Cruz Biotechnology, Dallas, TX; sc-15334), mouse MMP7 (R&D Systems, Minneapolis, MN; AF2967-SP), phospho-p44/42 MAPK (Erk1/2) (Thr202/204) (Cell Signaling Technology, Danvers, MA;

#9101). Secondary antibodies used included anti-rabbit IgG (H+L) Alexa Fluor 555 (Invitrogen, San Diego, CA; A-31572), anti-goat IgG (H+L) Alexa Fluor Plus 488 (Invitrogen; A32814). Nucleic acid was staining with DAPI (Sigma-Aldrich; F6057).

Establishment of Intestinal Organoid and Colon Organoid Cultures

Isolation of crypts from the jejunum of Lgr5-Cre; HER2^{V777L} Tg and HER2^{V777L} Tg littermate mice were performed as described.[25] Isolated intestinal crypts were embedded in Matrigel (BD Biosciences, San Jose, CA) and seeded in 6-well plates. The cells were overlaid with 2 mL/well basal culture medium (advanced Dulbecco's modified Eagle medium/F12 supplemented with penicillin/streptomycin, 10 mmol/L HEPES, Glutamax, $1 \times$ N2, $1 \times$ B27 (all from Thermo Fisher Scientific), and containing EGF (Sigma-Aldrich), noggin, and Rspo1 (noggin and R-spondin conditioned media were a gift from Blair Madison). For colon organoid generation, crypts were isolated from the proximal colon of Lgr5-Cre; HER2^{V777L} Tg and HER2^{V777L} Tg littermate mice and cultured in 50% L-WRN media as described previously.[26]

Transmission Electron Microscopy

For ultrastructural analyses, samples were fixed in 2% paraformaldehyde/2.5% glutaraldehyde (Polysciences, Warrington, PA) in 100 mM sodium cacodylate buffer, pH 7.2 for 2 hours at room temperature and then overnight at 4°C. Samples were washed in sodium cacodylate buffer at room temperature and postfixed in 1% osmium tetroxide (Polysciences) for 1 hour. Samples were then rinsed extensively in dH20 prior to en bloc staining with 1% aqueous uranyl acetate (Ted Pella, Redding, CA) for 1 hour. Following several rinses in dH20, samples were dehydrated in a graded series of ethanol and embedded in Eponate 12 resin (Ted Pella). Sections of 95 nm were cut with a Leica Ultracut UCT ultramicrotome (Leica Microsystems, Bannockburn, IL), stained with uranyl acetate and lead citrate, and viewed on a JEOL 1200 EX transmission electron microscope (JEOL USA, Peabody, MA) equipped with an AMT 8-MP digital camera and AMT Image Capture Engine V602 software (Advanced Microscopy Techniques, Woburn, MA).

Quantitative RT-PCR

RNA was isolated from the jejunum of the Lgr5-Cre; HER2^{V777L} Tg mice and 2 ug of RNA were reverse transcribed into complementary DNA using the complementary DNA reverse transcription kit (Applied Biosystems, Foster City, CA). qRT-PCR was performed with an ABI Prism 7300 Sequence Analyzer using SYBR green fluorescence probes. Quantification cycle (Cq) of genes of interest were normalized to the average Cq of 18s ribosomal RNA (reference gene) and expressed as relative mRNA levels. Primers were a gift from Matthew Ciorba[27] and primer sequences are the following:

Primer name and sequence
18s F GTAACCCGTTGAACCCCATT
18s R CCATCCAATCGGTAGTAGCG
mLgr5 F TGCCCATCACACTGTCACTGT
mLgr5 R CACCCTGAGCAGCATCCTG
mLrig1 F TTGAGGACTTGACGAATCTGC
mLrig1 R CTTGTTGTGCTGCAAAAAGAGAG
mAlpi F AGGACATCGCCACTCAACTC
mAlpi R GGTTCCAGACTGGTTACTGTCA
mAtoh1 F GGGGTTGTAGTGGACGAGC
mAtoh1 R CGTTGTTGAAGGACGGGATAAC
mMuc2 F ATGCCCACCTCCTCAAAGAC
mMuc2 R GTAGTTTCCGTTGGAACAGTGAA
mChgA F CCAAGGTGATGAAGTGCGTC
mChgA R GGTGTCGCAGGATAGAGAGGA
mLyz F GAGACCGAAGCACCGACTATG
mLyz R CGGTTTTGACATTGTGTTCGC
mDefcr5 F AGGCTGATCCTATCCACAAAACAG
mDefcr5 R TGAAGAGCAGACCCTTCTTGGC
mAxin2 F AACCTATGCCCGTTTCCTCT
mAxin2 R CTGGTCACCCAACAAGGAGT
mOlfm4 F GCCACTTTCCAATTTCAC
mOlfm4 R GAGCCTCTTCTCATACAC
mBmi1 F CCAATGAAGACCGAGGAGAA
mBmi1 R TTTCCGATCCAATCTGCTCT
mSI F GCTATCGCTCTTGTTGTGGTT
mSI R TTCCAGGACTAGGGGTTGAAG
mAlpi F AGGACATCGCCACTCAACTC
mAlpi R GGTTCCAGACTGGTTACTGTCA

Genomic Analysis of ERBB2 and APC Co-occurring Mutations

Mutations were extracted from The Cancer Genome Atlas Unified Ensemble MC3 Call Set.[14] Colon adenocarcinoma (COAD) or rectum adenocarcinoma (READ) patients were extracted from the MC3 mutation file, resulting in a total of 559 patients with 223,860 mutations (excluding the following mutation types: Silent, Intron, RNA, 5′ flank, 3′ flank, IGR, translation start site, 3′ UTR, and 5′ UTR).

Statistical Analysis

Data are presented as means and SEM. The Student t test and the Mann-Whitney U test was used to analyze data with 2 groups. For statistical analysis, GraphPad Prism version 7 (GraphPad Software, San Diego, CA) was used. A P value <.05 was considered statistically significant. All authors had access to the study data and reviewed and approved the final manuscript.

References

1. Tang X, Liu H, Yang S, Li Z, Zhong J, Fang R. Epidermal growth factor and intestinal barrier function. Mediators Inflamm 2016;2016:1927348.
2. Iqbal N, Iqbal N. Human epidermal growth factor receptor 2 (HER2) in cancers: overexpression and therapeutic implications. Mol Biol Int 2014;2014:852748.
3. Sigismund S, Avanzato D, Lanzetti L. Emerging functions of the EGFR in cancer. Mol Oncol 2018;12:3–20.

4. The Cancer Genome Atlas Consortium. Comprehensive molecular characterization of human colon and rectal cancer. Nature 2012;487:330–337.

5. Kavuri SM, Jain N, Galimi F, Cottino F, Leto SM, Migliardi G, Bose R. HER2 activating mutations are targets for colorectal cancer treatment. Cancer Discov 2015;5:832–841.

6. Roberts RB, Min L, Washington MK, Olsen SJ, Settle SH, Coffey RJ, Threadgill DW. Importance of epidermal growth factor receptor signaling in establishment of adenomas and maintenance of carcinomas during intestinal tumorigenesis. Proc Natl Acad Sci U S A 2002; 99:1521–1526.

7. Zhang Y, Dubé PE, Washington MK, Yan F, Polk DB. ErbB2 and ErbB3 regulate recovery from dextran sulfate sodium-induced colitis by promoting mouse colon epithelial cell survival. Lab Invest 2012;92:437–450.

8. Lee D, Yu M, Lee E, Kim H, Yang Y, Kim K, Pannicia C, Kurie JM, Threadgill DW. Tumor-specific apoptosis caused by deletion of the ERBB3 pseudo-kinase in mouse intestinal epithelium. J Clin Invest 2009;119:2702–2713.

9. Almohazey D, Lo YH, Vossler CV, Simmons AJ, Hsieh JJ, Bucar EB, Schumacher MA, Hamilton KE, Lau KS, Shroyer NF, Frey MR. The ErbB3 receptor tyrosine kinase negatively regulates Paneth cells by PI3K-dependent suppression of Atoh1. Cell Death Diff 2017;24:855–865.

10. Barker N, van Es J, Kuipers J, Kujala P, van den Born M, Cozijnsen M, Haegebarth A, Korving J, Begthel H, Peters PJ, Clevers H. Identification of stem cells in small intestine and colon by marker gene Lgr5. Nature 2007; 449:1003–1007.

11. Barker N, Clevers H. (2010). Lineage tracing in the intestinal epithelium. Curr Protoc Stem Cell Biol 2010, Chapter 5:Unit5A.4.

12. Mahoney ZX, Thaddeus S, Stappenbeck TS, Miner JH. Laminin α5 influences the architecture of the mouse small intestine mucosa. J Cell Sci 2008;121:2493–2502.

13. Stappenbeck TS, Gordon JI. Rac1 mutations produce aberrant epithelial differentiation in the developing and adult mouse small intestine. Development 2000; 127:2629–2642.

14. Ellrott K, Bailey MH, Saksena G, Covington KR, Kandoth C, Stewart C, Hess J, Ma S, Chiotti KE, McLellan M, Sofia HJ, Hutter C, Getz G, Wheeler D, Ding L. MC3 Working Group; Cancer Genome Atlas Research Network [dataset]. Cell Syst 2018;6:271–281.

15. Bose R, Kavuri SM, Searleman AC, Shen W, Shen D, Koboldt DC, Monsey J, Goel N, Aronson AB, Li S, Ma CX, Ding L, Mardis ER, Ellis MJ. Activating HER2 mutations in HER2 gene amplification negative breast cancer. Cancer Discov 2013;3:224–237.

16. Mishra R, Alanazi S, Yuan L, Solomon T, Thaker TM, Jura N, Garrett JT. Activating HER3 mutations in breast cancer. Oncotarget 2018;9:27773–27788.

17. Feng Y, Bommer GT, Zhao J, Green M, Sands E, Zhai Y, Brown K, Burberry A, Cho KR, Fearon ER. Mutant KRAS promotes hyperplasia and alters differentiation in the colon epithelium but does not expand the presumptive stem cell pool. Gastroenterology 2011; 141:1003–1013.e10.

18. Wong VW, Stange DE, Page ME, Buczacki S, Wabik A, Itami S, van de Wetering M, Poulsom R, Wright NA, Trotter MW, Watt FM, Winton DJ, Clevers H, Jensen KB. Lrig1 controls intestinal stem-cell homeostasis by negative regulation of ErbB signalling. Nat Cell Biol 2012; 14:401–408.

19. Johnson E, Seachrist DD, DeLeon-Rodriguez CM, Lozada KL, Miedler J, Abdul-Karim FW, Keri RA. HER2/ErbB2-induced breast cancer cell migration and invasion require p120 catenin activation of Rac1 and Cdc42. J Biol Chem 2010;285:29491–29501.

20. Melendez J, Liu M, Sampson L, Akunuru S, Han X, Vallance J, Witte D, Shroyer N, Zheng Y. Cdc42 coordinates proliferation, polarity, migration, and differentiation of small intestinal epithelial cells in mice. Gastroenterology 2013;145:808–819.

21. VanDussen KL, Carulli AJ, Keeley TM, Pate SR, Puthoff BJ, Magness ST, Tran IT, Maillard I, Siebe C, Kolterud A, Grosse AS, Gumucio DL, Ernst SA, Tsai Y-H, Dempsey PJ, Samuelson LC. Notch signaling modulates proliferation and differentiation of intestinal crypt base columnar stem cells. Development 2012;139:488–497.

22. Soriano P. Generalized lacZ expression with the ROSA26 Cre reporter strain. Nat Genet 1999;(21):70–71.

23. Madison BB, Dunbar L, Qiao XT, Braunstein K, Braunstein E, Gumucio DL. cis elements of the villin gene control expression in restricted domains of the vertical (crypt) and horizontal (duodenum, cecum) axes of the intestine. J Biol Chem 2002;277:33275–33283.

24. Wang Y, Chiang IL, Ohara TE, Fujii S, Cheng J, Muegge BD, Ver Heul A, Han ND, Lu Q, Xiong S, Chen F, Lai CW, Janova H, Wu R, Whitehurst CE, VanDussen KL, Liu TC, Gordon JI, Sibley LD, Stappenbeck TS. Long-term culture captures injury-repair cycles of colonic stem cells. Cell 2019;179:1144–1159.

25. Sato T, Clevers H. Primary mouse small intestinal epithelial cell cultures. Methods Mol Biol 2013;945:319–328.

26. Miyoshi H, Stappenbeck TS. In vitro expansion and genetic modification of gastrointestinal stem cells in spheroid culture. Nat Protoc 2013;8:2471–2482.

27. Alvarado DM, Chen B, Iticovici M, Thaker AI, Dai N, VanDussen KL, Shaikh N, Lim CK, Guillemin GJ, Tarr PI, Ciorba MA. Epithelial indoleamine 2,3-dioxygenase 1 modulates aryl hydrocarbon receptor and notch signaling to increase differentiation of secretory cells and alter mucus-associated microbiota. Gastroenterology 2019;157:1093–1108.

Correspondence
Address requests for correspondence to: Ron Bose, MD, PhD, Washington University School of Medicine, 4515 McKinley Avenue, Campus Box 8069, St. Louis, Missouri 63110. e-mail: rbose@wustl.edu; fax: (314) 747-9320.

CRediT Authorship Contributions

Elisa Murray (Data curation: Lead; Formal analysis: Lead; Investigation: Lead; Methodology: Lead; Writing – original draft: Lead; Writing – review & editing: Equal)

Xiaoqing Cheng, PhD (Formal analysis: Equal; Investigation: Supporting; Writing – original draft: Supporting)

Anagha Krishna, PhD (Data curation: Supporting; Data Acquisition: Supporting)

Xiaohua Jin, MD (Investigation: Supporting; Methodology: Supporting)

Takahiro E. Ohara (Resources: Equal; Writing – review & editing: Supporting; Data Acquisition: Supporting)

Thaddeus S. Stappenbeck, MD, PhD (Conceptualization: Supporting; Resources: Equal; Writing – review & editing: Supporting)

Ron Bose, MD, PhD (Conceptualization: Lead; Funding acquisition: Lead; Supervision: Lead; Writing – review & editing: Equal)